Available online at www.sciencedirect.com
SCIENCE DIRECT®
Journal of Magnetic Resonance 175 (2005) 201–209
JMR Journal of Magnetic Resonance
www.elsevier.com/locate/jmr

Crossed-coil detection of two-photon excited nuclear quadrupole resonance

Philip T. Eles, Carl A. Michal *

Department of Physics and Astronomy, University of British Columbia, 6224 Agricultural Road, Vancouver, Canada V6T 1Z1

Received 21 February 2005; revised 5 April 2005
Available online 12 May 2005

Abstract

Applying a recently developed theoretical framework for determining two-photon excitation Hamiltonians using average Hamiltonian theory, we calculate the excitation produced by half-resonant irradiation of the pure quadrupole resonance of a spin-3/2 system. This formalism provides expressions for the single-quantum and double-quantum nutation frequencies as well as the Bloch–Siegert shift. The dependence of the excitation strength on RF field orientation and the appearance of the free-induction signal along an axis perpendicular to the excitation field provide an unmistakable signature of two-photon excitation. We demonstrate single- and double-quantum excitation in an axially symmetric system using ^{35}Cl in a single crystal of potassium chlorate ($\omega_Q = 28$ MHz) with crossed-coil detection. A rotation plot verifies the orientation dependence of the two-photon excitation, and double-quantum coherences are observed directly with the application of a static external magnetic field.

Keywords: Nuclear quadrupole resonance; Two-photon excitation; Average Hamiltonian theory; Crossed-coil detection; Half-resonance RF; Receiver dead-time; Probe ring-down

1. Introduction

Multi-photon excitation is a general consequence of higher order perturbation theory and is well understood, typically in the context of atomic electrons coupled to a radiation field as is the case in many optics experiments [1]. In early cw optics [1], electron paramagnetic resonance (EPR) [2,3] and nuclear magnetic resonance (NMR) [4,5] experiments, multi-photon excitation was described by absorption cross-sections or transition probabilities calculated using time-dependent perturbation theory. Where phase sensitive excitation and detection is important, as in pulsed EPR and NMR as well as more recent coherent optics experiments [6], coherent descriptions of multi-photon excitation are necessary. Coherent multi-photon excitation has been described in a number of different formalisms: vectorially by Bloch equations [7,8], by rotating frame transformations [9–11], by second quantization [12,13], or by Floquet theory [14–17]. Recently, we presented a new approach [18] based on average Hamiltonian theory [19].

Practical applications of multi-photon excitation abound in optics [20] and in EPR [17] where various combinations of linearly and circularly polarized microwave and radiofrequency irradiations have been used to produce two-, three-, and four-photon excitation. Due to the inherent insensitivity of NMR and nuclear quadrupole resonance (NQR) experiments, multi-photon processes have not been widely exploited to date. Pulsed multi-photon excitation of NMR has been demonstrated experimentally [15,16,21] but has largely been limited to the absorption of an odd number of photons, or to the excitation of unobservable $|\Delta m| > 1$ coherences. Only recently have we demonstrated practical two-pho-

* Corresponding author. Fax: +1 604 822 5324.
E-mail address: michal@physics.ubc.ca (C.A. Michal).

1090-7807/$ - see front matter © 2005 Elsevier Inc. All rights reserved.
doi:10.1016/j.jmr.2005.04.006

ton excitation of directly observable single-quantum coherences by applying an RF field with components both parallel and perpendicular to the static magnetic field [10,18].

A general result of monochromatic n-photon excitation of a resonance line with a transition frequency ω_0 is that the nutation rate is proportional to $(\gamma B_1)^n/\omega_0^{n-1}$, where γ is the gyromagnetic ratio of the nucleus and B_1 is the strength of the applied RF field. The nutation rate is thus significantly suppressed compared to on-resonance ($n = 1$) excitation, but the suppression is less severe when γ is reasonably large and the resonance frequency is low due to a weak static external field (NMR) or quadrupolar coupling (NQR).

The production of observable coherences by far off-resonant irradiation has a number of distinct advantages over on-resonant irradiation including the complete elimination of receiver dead-time, allowing simultaneous excitation and detection [10,18]. This benefit of two-photon excitation is of greater importance at low frequencies where long receiver dead times due to probe ringing may outlast the free induction signal. For this reason, the application of two-photon excitation to nuclear quadrupole resonance has been proposed [11]. The work of Sauer et al. [22,23] in the case of a 3-level NQR system (a spin-1 nucleus with $\eta \neq 0$), achieved a similar goal, where excitation at two of the transition frequencies allowed detection at the third. That work differs from our two-photon approach as it involves generating a single quantum coherence between two levels via a third. In our approach no additional levels are required and the irradiation frequency does not correspond to any transition.

In this paper, we treat two-photon excitation of nuclear quadrupole resonance, first for an axially symmetric spin-3/2 nucleus, with average Hamiltonian theory as described in [18]. Results of the theory applied to the more general but less intuitive case without axial symmetry are then described. The current treatment builds on our previous demonstration of two-photon NQR [11] by providing a more complete description of the two-photon excitation Hamiltonian as well as a quantitative comparison of experiment with theory for the important $\eta = 0$ case. The current formalism reproduces the single-quantum excitation terms of the effective Hamiltonian found with the earlier rotating frame approach, and further provides expressions for the Bloch–Siegert shift and for terms that directly generate double-quantum coherences. For the axially symmetric case, we experimentally confirm the angular dependence of the two-photon single-quantum excitation, demonstrate that observable signal arises perpendicular to the excitation axis, and directly observe the double-quantum coherences generated by the newly predicted terms by application of a weak static external magnetic field.

2. Theory

In the principle axis system (PAS) of the quadrupole interaction, the Hamiltonian of a single spin-3/2 nucleus in an external electric field gradient and a linear RF magnetic field is

$$\mathcal{H} = \mathcal{H}_Q + \mathcal{H}_{\mathrm{RF}} \tag{1}$$

$$= \frac{\omega_Q}{6}\left[3I_z^2 - I(I+1) + \eta(I_x^2 - I_y^2)\right] + \left(\omega_x I_x + \omega_y I_y + \omega_z I_z\right)\cos\omega_{\mathrm{RF}} t, \tag{2}$$

where $\omega_Q = e^2qQ/2$ is the strength of the quadrupolar interaction, η is the asymmetry parameter of the electric field gradient, and $\omega_x = \gamma(\vec{B}_1 \cdot \hat{x})$, $\omega_y = \gamma(\vec{B}_1 \cdot \hat{y})$, and $\omega_z = \gamma(\vec{B}_1 \cdot \hat{z})$ are the projections of the RF field onto the x, y, and z axes of the PAS respectively.

Following the prescription for calculating the two-photon excitation Hamiltonian as set out in [18], we transform Eq. (2) into an interaction representation using the unitary operator $U = \mathrm{e}^{\mathrm{i}\mathcal{H}_Q t}$ such that the static quadrupolar Hamiltonian is removed.

2.1. Two-photon excitation of NQR for a spin-3/2 nucleus with $\eta = 0$

Specializing now to the axially symmetric case where the interaction frame transformation is straightforward, and choosing the x axis so that the RF lies in the x–z plane (making $\omega_y = 0$), we find an effective Hamiltonian given by

$$\mathcal{H}_{\mathrm{eff}} = \left[\omega_x U^\dagger I_x U + \omega_z I_z\right]\cos\omega_{\mathrm{RF}} t \tag{3}$$

$$= \left[\sqrt{3}\omega_x\left(\cos\omega_Q t\left(I_x^{1-2} + I_x^{3-4}\right) + \sin\omega_Q t \times\left(I_y^{1-2} - I_y^{3-4}\right)\right) + 2\omega_x I_x^{2-3} + \omega_z I_z\right]\cos\omega_{\mathrm{RF}} t, \tag{4}$$

where Eq. (4) has been written in terms of fictitious spin-1/2 operators [24]. In the axially symmetric case, the Zeeman states, quantized along the z axis, are eigenstates of the system, and the superscripts $1 \to 4$ correspond to the states $|3/2\rangle$, $|1/2\rangle$, $|-1/2\rangle$, and $|-3/2\rangle$ respectively.

The time-averaged effects resulting from this time-dependent Hamiltonian can be described by average Hamiltonian theory via the Magnus expansion [25], the first two terms of which are

$$\mathcal{H}^{(0)} = \frac{1}{t}\int_0^t \mathrm{d}t' \mathcal{H}_{\mathrm{eff}}(t'), \tag{5}$$

$$\mathcal{H}^{(1)} = \frac{-\mathrm{i}}{2t}\int_0^t \mathrm{d}t' \int_0^{t'} \mathrm{d}t''[\mathcal{H}_{\mathrm{eff}}(t'), \mathcal{H}_{\mathrm{eff}}(t'')]. \tag{6}$$

For irradiation at half-resonance ($\omega_{\mathrm{RF}} = \omega_Q/2$), the first non-zero term in the Magnus expansion is the first order term, which, calculated for convenience in the limit

$t \to \infty$, yields the time-independent two-photon excitation Hamiltonian:

$$\mathcal{H}^{(1)} = \omega_{\mathrm{BS}}^{0Q}\left(3I_z^2 - I(I+1)\right)/6 + \omega_{\mathrm{nut}}^{1Q}\left(I_x^{1-2} - I_x^{3-4}\right) + \omega_{\mathrm{nut}}^{2Q}\left(I_x^{1-3} + I_x^{2-4}\right), \quad (7)$$

where

$$\omega_{\mathrm{BS}}^{0Q} = -\frac{\omega_x^2}{\omega_Q} = -\frac{(\gamma B_1)^2}{\omega_Q}\sin^2\alpha, \quad (8)$$

$$\omega_{\mathrm{nut}}^{1Q} = \frac{\sqrt{3}}{2}\frac{\omega_x\omega_z}{\omega_Q} = \frac{\sqrt{3}}{2}\frac{(\gamma B_1)^2}{\omega_Q}\cos\alpha\sin\alpha, \quad (9)$$

$$\omega_{\mathrm{nut}}^{2Q} = -\frac{\sqrt{3}}{2}\frac{\omega_x^2}{\omega_Q} = -\frac{\sqrt{3}}{2}\frac{(\gamma B_1)^2}{\omega_Q}\sin^2\alpha, \quad (10)$$

and α is the angle between the quadrupolar symmetry axis and the RF coil. The Hamiltonian in Eq. (7) has been arranged to group together the zero-, single-, and double-quantum terms. The last two are responsible for nutation into single- and double-quantum coherences whereas the first term, proportional to the quadrupolar interaction Hamiltonian, is a resonance offset analogous to the Bloch–Siegert shift in NMR [26]. This Bloch–Siegert shift is typically small (approximately 100 Hz for the experiments presented here) and is simply a resonance offset that is effective only when the RF field is present.

The single-quantum term in Eq. (7) results in $\Delta m = \pm 1$ transitions between the $|\pm 3/2\rangle$ and $|\pm 1/2\rangle$ states that are due to the absorption of one transverse and one longitudinal photon (see Fig. 1). The resulting single-quantum coherence leads to directly observable signal. We use the terms longitudinal and transverse to describe photons according to the orientation of the corresponding RF field component with respect to the z axis in the PAS. These photons carry zero or one unit of angular momentum and correspond to the zero (I_z) or single (I_x and I_y) quantum operators of Eq. (2).

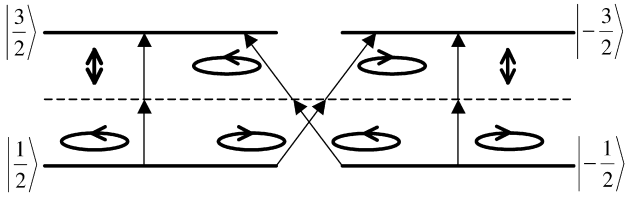

Fig. 1. The single- and double-quantum terms in the two-photon Hamiltonian represent absorption of one longitudinal (↕) and one transverse (○ or ◌) photon or two transverse photons resulting in a $\Delta m = \pm 1$ and $\Delta m = \pm 2$ transitions respectively. The latter does not result in observable signal in a zero field NQR experiment. By contrast, on-resonance excitation with a single photon only couples the $\Delta m = \pm 1$ states.

The double-quantum term in Eq. (7) that addresses the $|\pm 3/2\rangle$ and $|\mp 1/2\rangle$ transitions (with $\Delta m = \pm 2$ due to absorption of two transverse photons) does not lead to a state that is observable under evolution due solely to the quadrupolar interaction. This double-quantum coherence does contribute to the observed signal if a static magnetic field is present during detection.

2.2. Observable free induction decay for $\eta = 0$

The evolution of the system under two-photon irradiation is complicated by the presence of the double-quantum terms of Eq. (7), as they interfere with the simple nutation produced by the single-quantum terms. In the absence of a static magnetic field, the free induction signal, $\langle\vec{I}\rangle$, along an arbitrary direction in the PAS of the quadrupolar interaction after a half-resonant pulse of duration τ is given by

$$\langle\vec{I}(t>\tau)\rangle = \mathrm{Tr}\{\rho(t)\vec{I}\} = \mathrm{Tr}\left\{e^{i\mathcal{H}^{(1)}\tau}\rho(0)e^{-i\mathcal{H}^{(1)}\tau}U\vec{I}U^\dagger\right\}. \quad (11)$$

Assuming that the initial density matrix is $\rho(0) \propto \mathcal{H}_Q$, the above evolution yields:

$$\langle\vec{I}\rangle \propto \cos\alpha\sin\left(\frac{\omega_{\mathrm{nut}}^{1Q}\tau}{\cos\alpha}\right)\cos(\omega_Q t)\hat{y}, \quad (12)$$

revealing that observable signal appears only along the y axis, which is perpendicular to both the excitation axis and the symmetry axis of the quadrupolar interaction. The interference of the double-quantum term accelerates $\omega_{\mathrm{nut}}^{1Q}$ by a factor of $1/\cos\alpha$ while reducing the amplitude of the observed signal by $\cos\alpha$. In the limit of short pulses ($\omega_{\mathrm{nut}}\tau \ll 1$), and assuming detection along the Z axis in the lab frame, the amplitude of the detected signal, S, is

$$S \propto \omega_{\mathrm{nut}}^{1Q}\tau(\hat{y}\cdot\hat{Z}) = \frac{\sqrt{3}}{2}\frac{\omega_x\omega_z}{\omega_Q}\tau(\hat{y}\cdot\hat{Z}), \quad (13)$$

where the interference of the double-quantum terms is no longer apparent.

2.3. The case of $\eta \neq 0$

The calculation of the two-photon excitation Hamiltonian for a spin-3/2 system with non-zero asymmetry parameter is similar to the $\eta = 0$ case and is reproduced in full in Appendix A. The result is

$$\mathcal{H}^{(1)} = \Omega_{\mathrm{BS}}^{0Q}\left[3I_z^2 - I(I+1) + \eta(I_x^2 - I_y^2)\right]/6 + \Omega_{xz}^{1Q}(I_x^{1-2} - I_x^{3-4}) + \Omega_{yz}^{1Q}(I_y^{1-2} - I_y^{3-4}) + \Omega_{xy}^{1Q}(I_y^{1-3} + I_y^{2-4}) + \Omega^{2Q}(I_x^{1-3} + I_x^{2-4}), \quad (14)$$

where

$$\Omega_{\mathrm{BS}}^{0Q} = \left\{(4\kappa^2+3)(\omega_x^2+\omega_y^2) + \tfrac{\sqrt{3}}{2}\kappa(3\kappa^2+1)(\omega_x^2-\omega_y^2) - 2\kappa^2\omega_z^2\right\}/3\xi^3\omega'_Q, \tag{15}$$

$$\Omega_{xz}^{1Q} = -\frac{\omega_x\omega_z(3\kappa+\sqrt{3})}{2\xi\omega'_Q}, \tag{16}$$

$$\Omega_{yz}^{1Q} = \frac{\omega_y\omega_z(3\kappa-\sqrt{3})}{2\xi\omega'_Q}, \tag{17}$$

$$\Omega_{xy}^{1Q} = \frac{\sqrt{3}\omega_x\omega_y}{\xi\omega'_Q}, \tag{18}$$

$$\Omega^{2Q} = \frac{-\kappa(\omega_x^2+\omega_y^2) - \frac{\sqrt{3}}{2}(\kappa^2-1)(\omega_x^2-\omega_y^2) + 2\kappa\omega_z^2}{\xi\omega'_Q}, \tag{19}$$

and $\kappa = \eta/\sqrt{3}$, $\xi = \sqrt{1+\kappa^2}$, and $\omega'_Q = \xi\omega_Q$. The resulting excitation Hamiltonian is qualitatively similar to the $\eta = 0$ case in that it consists of a Bloch–Siegert shift and single- and double-quantum excitation terms. Eq. (14) reduces to Eq. (7) for the symmetric case of $\eta = 0$, if the x axis is chosen so that the RF again lies in the x–z plane.

If $\eta \neq 0$, the Zeeman states are no longer eigenstates of the system and the excitation Hamiltonian terms we have labeled as single- and double-quantum do not produce states that are properly described as single- or double-quantum coherences. Furthermore, the evolution of the density matrix under such irradiation is non-trivial. An intuition for the evolution of the system may be obtained by considering short pulses ($\mathcal{H}^{(1)}\tau \ll 1$), where each term in Eq. (14) can be considered independently. The result (presented in full in Appendix A) is that observable signal is generated by the second, third or fourth terms of Eq. (14) when the RF has components along any two of the quadrupolar axes, with the signal appearing along the third axis. However, the vector sum of the signals generated by each of the three terms points in a direction perpendicular to the excitation axis (see Eq. (A.8)). Therefore, even in the $\eta \neq 0$ case, a second coil is required for detection, in contradiction to a claim made in an earlier paper [11]. As expected, the first term in Eq. (14) (the Bloch–Siegert shift term), which has been grouped in such a way as to be proportional to the quadrupolar interaction, generates no observable signal. Also, the fifth term generates no observable signal as it is the equivalent of a double-quantum excitation.

Further intuition into the $\eta \neq 0$ case can be gained from the $\eta = 0$ case where we discussed the concept of excitation through absorption of longitudinal and transverse photons. Because, in the $\eta \neq 0$ case, none of the quadrupolar axes is preferred, excitation along any one of the axes should be possible, requiring the absorption of two photons: one transverse and one longitudinal with respect to that axis to generate observable coherences, or two transverse photons to generate an unobservable coherence. This description is born out in the geometric factors in Eqs. (15)–(19).

In our treatment, the linear RF field applied along an arbitrary direction in the quadrupolar PAS can be decomposed into a set of transverse and longitudinal fields capable of supplying both transverse and longitudinal photons along any, depending on crystal orientation, of the quadrupolar axes. In other experimental configurations, where independent transverse and longitudinal fields may be applied in arbitrary directions, only certain terms in Eq. (14) may survive.

3. Methods

A 300 mg potassium chlorate ($KClO_3$) single crystal (of approximate dimensions $3 \times 8.25 \times 9.5$ mm) was grown by slow evaporation of a saturated solution. Potassium chlorate forms a monoclinic crystal with two molecules per unit cell in the space group $P2_1/m$ [27]. The symmetry axis of the quadrupolar interaction is perpendicular to the plane defined by the three oxygens [28], which form a nearly tetrahedral arrangement with the chlorine atom. The two molecular sites are related by an inversion center and therefore are indistinguishable in our magnetic resonance experiments. The symmetry axis of the quadrupolar interaction makes an angle of $\beta = 57°$ with the crystal c axis, which lies perpendicular to the one large crystal face.

All NQR spectra were acquired on a home-built spectrometer [29] in a home-built wideline probe with a 9.6 mm (inner diameter) solenoid coil resonant at 14 MHz inside a larger saddle coil resonant at 28 MHz. Thus, for two-photon excitation, the excitation and detection axes were orthogonal, whereas for on-resonance excitation, the saddle coil was used for both excitation and detection. Those two-photon spectra obtained with a single excitation and detection coil were acquired with the probe circuit rebuilt so that the solenoid coil was doubly resonant at 14 and 28 MHz.

Unless otherwise stated, two-photon spectra were collected after 100 μs of RF irradiation, while on-resonance excitation spectra were obtained after a π/2 pulse of 13 μs, with approximately 600 W of RF power in both cases. To determine the proper first order phase correction for the two-photon excited spectra, on-resonance excited spectra were also collected with weak 100 μs pulses. A home-built high-power 15 MHz lowpass filter, which attenuated on-resonance RF by 80 dB compared to half-frequency RF, was used to minimize any on-resonance excitation by second harmonic generated in the amplifier. Any 28 MHz RF that may have been generated was below the detection level of a digital oscilloscope (<0.1 mW) when coupled directly to the probe's

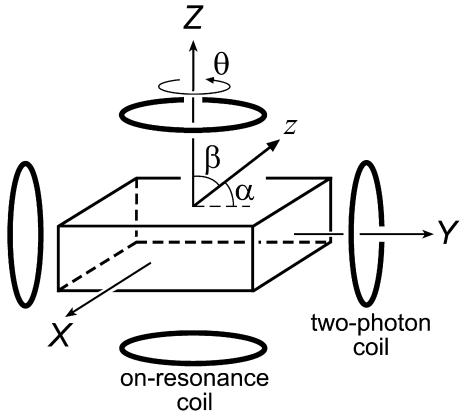

Fig. 2. Schematic of crystal orientation in the lab frame, with the Z axis defined to be along the on-resonance coil axis and the Y axis along the two-photon RF coil. The symmetry axis of the quadrupolar interaction, z, makes an angle of $\beta = 57°$ with the lab Z axis. α is defined to be the angle between z and the Y axis and depends on the rotation of the crystal about the Z axis by an angle θ defined to be zero when z is in the Y–Z plane.

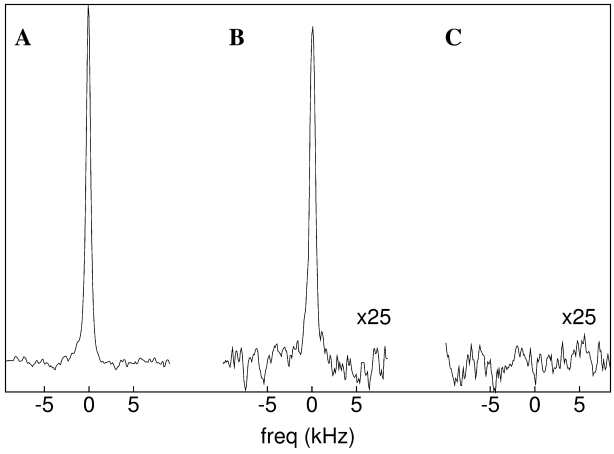

Fig. 3. ^{35}Cl NQR spectra of $KClO_3$. (A) Spectrum acquired following an on-resonance excitation pulse with excitation and detection in the same coil. (B and C) Spectra acquired following a pulse at half the resonance frequency with the RF applied along (B) $\alpha = 53.6°$ ($\theta = 45°$) and (C) $\alpha = 90°$ ($\theta = 90°$). Detection was along an axis perpendicular to the direction of excitation as described in the text.

28 MHz channel during a half-resonance RF pulse. To cancel the earth's magnetic field, or to generate an external field, the probe was placed inside a 20 cm diameter Helmholtz coil that was powered by a computer-controlled power supply (Circuit-Test Electronics, Burnaby, Canada). The field was characterized by a hand-held Hall effect Gaussmeter (F.W. Bell, Orlando, FL).

Rotation plots were obtained with a smaller (170 mg) $KClO_3$ single crystal mounted onto a poly(tetrafluoroethylene) (PTFE) holder inside the RF coil with the crystal c axis colinear with the on-resonance coil axis (see Fig. 2). Sample rotation about the c axis was achieved by a spectrometer controlled stepper motor that was coupled to the PTFE holder via a plastic gear and chain set. Each spectrum is the average of 1024 scans taken one per second.

The temperature sensitivity of the quadrupole coupling constant (approximately -5.7 kHz/K near room temperature [30]) was significant. Temperature fluctuations of less than 0.1° would result in frequency shifts greater than the spectral linewidth. High-power RF irradiation during two-photon excitation resulted in transient temperature fluctuations at the beginning of an acquisition, requiring several hundred scans be discarded before signal averaging was commenced.

4. Results and discussion

4.1. Single-quantum coherences and rotation plots

The ^{35}Cl NQR spectrum of potassium chlorate excited on-resonance is shown in Fig. 3A. A two-photon spectrum, shown in Fig. 3B, was obtained with detection along an axis perpendicular to the excitation axis, following an excitation pulse applied at half the NQR frequency.

The relative integrated intensities of the peaks in Figs. 3A and B indicate a tip angle of 2.64° for the 100 μs two-photon pulse, or a nutation frequency of $\omega_{\text{nut}}^{1Q} = 2\pi(73\text{ Hz})$. The strength of the 14 MHz RF field, calibrated by measuring the nutation rate of ^{14}N spins in a saturated solution of glycine on an MSL200 (Bruker) NMR spectrometer ($\omega_0 = 14.451$ MHz), was measured to be $B_1 = 23.0$ mT. According to Eq. (9), such a B_1 would result in a two-photon nutation frequency of $\omega_{\text{nut}}^{1Q} = 2\pi(87\text{ Hz})$, in good agreement with the measured value.

Fig. 3C shows the two-photon excited spectrum of $KClO_3$ with the crystal rotated such that the excitation RF is oriented along an axis perpendicular to the quadrupole axis ($\alpha = 90°$, $\theta = 90°$). As predicted from Eqs. (7) and (9), no excitation was observed with the excitation coil in this orientation. Similarly, for $\theta = 0°$ (data not shown), when the symmetry axis was in the plane defined by the excitation and detection coils, no signal was observed because the free induction signal appears along a direction perpendicular to the detection coil. Based on the angular dependence of ω_{nut}^{1Q}, during a complete rotation about Z ($\theta = 0 \rightarrow 2\pi$), there should be four crystal orientations at which no signal can be observed. In fact, for the coil geometry used in these experiments the expected signal, as given by Eq. (13), is

$$S \propto \frac{(\gamma B_1)^2 \tau}{\omega_Q} \sin^2\beta \sin 2\theta \sqrt{1 - \sin^2\beta \cos^2\theta}. \tag{20}$$

Indeed for two-photon excitation (Fig. 4B), we observe the two-photon excited intensity undergo two full periods through one rotation of the crystal as predicted. By contrast, the on-resonance excited signal intensity

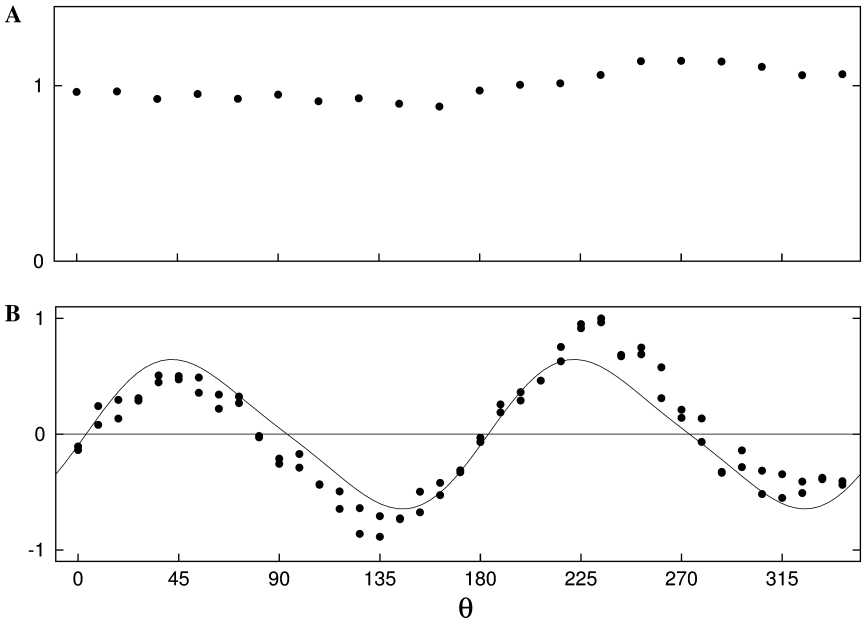

Fig. 4. Rotation plot of $KClO_3$. (A) Integrated peak intensity for on-resonance excitation with a $\pi/2$ pulse. (B) Integrated peak intensity after a 100 μs two-photon excitation pulse. For (B), the sample was rotated through two complete revolutions. Deviations from the expected intensities are attributed to the movement of sample within the coil.

is expected to be independent of the rotation angle as is observed in Fig. 4A.

4.2. Excitation and detection of double-quantum coherences

The double-quantum term in Eq. (7) generates coherences that are unobservable in a pure quadrupole resonance experiment where $\Delta m \neq \pm 1$ transitions are forbidden. To demonstrate that these coherences do exist, a weak static magnetic field was applied.

A degenerate perturbation theory treatment [31] shows that the static field mixes the $|\pm 1/2\rangle$ states (see Fig. 5) so that as long as the magnetic field is not colinear with the quadrupolar symmetry axis, the Zeeman states are no longer eigenstates of the system, and any double-quantum coherences of the form $a\ |\pm 3/2\rangle + b\ |\mp 1/2\rangle$ generated by two-photon excitation are observable. Level splittings due to the magnetic field result in a set of two doublets, with the inner doublet (known as the α lines) due to $|\pm 3/2\rangle$ to $|\mp\rangle$ transitions and the outer doublet (the β lines) due to $|\pm 3/2\rangle$ to $|\pm\rangle$ transitions.

In general, if both the single- and double-quantum terms were to contribute to excitation, in the limit of short pulses, the resulting spectrum would be an admixture of the spectra that would be obtained from each term. However, from Eqs. (9) and (10) the angular dependence is different for the two terms with the single-quantum term requiring projections of the excitation field both parallel and perpendicular to the z axis of the quadrupolar PAS, whereas the double-quantum term requires only a perpendicular projection. Thus, by setting

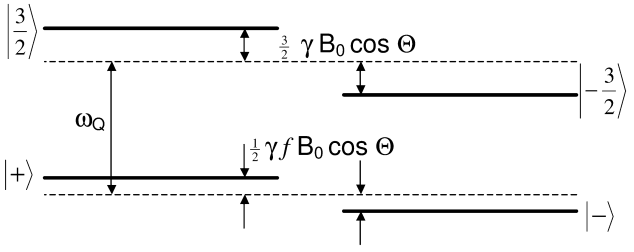

Fig. 5. Energy level diagram for an axially symmetric quadrupolar interaction of a spin-3/2 nucleus perturbed to first order by a weak external magnetic field, B_0, oriented at an angle Θ to the symmetry axis of the quadrupolar interaction. The $|\pm 1/2\rangle$ states are mixed such that $|+\rangle = \cos\delta\ |1/2\rangle + \sin\delta\ |-1/2\rangle$ and $|-\rangle = -\sin\delta\ |1/2\rangle + \cos\delta\ |-1/2\rangle$, where $\tan\delta = \sqrt{(f-1)/(f+1)}$ and $f = \sqrt{1+(I+1/2)^2\tan^2\Theta}$. The transitions $|\pm 3/2\rangle \rightarrow |\pm\rangle$ and $|\pm 3/2\rangle \rightarrow |\mp\rangle$ yield the well known α and β lines with splittings $\Delta\omega_\alpha = (3-f)\cos\Theta$ and $\Delta\omega_\beta = (3+f)\cos\Theta$ and relative intensities $\cos\delta$ and $\sin\delta$ [31].

$\alpha = 90°$, only the double-quantum term will contribute to excitation and in the absence of a static magnetic field no signal should be observed.[1]

^{35}Cl NQR spectra of $KClO_3$ with the excitation RF perpendicular to the symmetry axis of the quadrupolar interaction are shown in Fig. 6. For on-resonance excita-

[1] In the present analysis, it has been assumed that the magnetic field is weak ($\gamma B_0 \tau \ll 1$), so that the static field may be neglected during excitation, acting only during the subsequent evolution time. A more careful analysis must be performed if this condition is not fulfilled or if a more quantitative agreement between experiment and theory is necessary. In such circumstances, numerical methods such as a stepwise integration of the Bloch equations may be more practical.

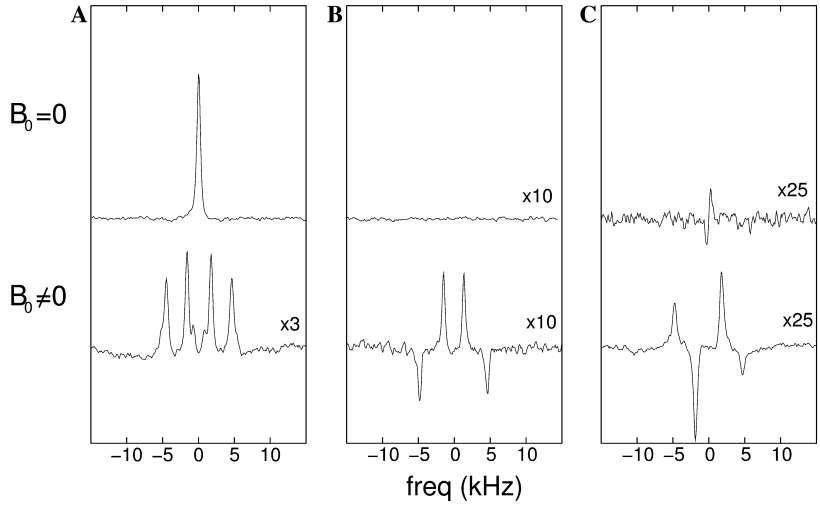

Fig. 6. ^{35}Cl NQR spectra of $KClO_3$ with excitation RF perpendicular to the symmetry axis of the quadrupolar interaction. Top spectra are in zero external magnetic field, while an external magnetic field of 8 G was applied to bottom spectra to render double-quantum coherences observable. (A) On-resonance excitation, (B) two-photon excitation with crossed-coil detection, and (C) two-photon excitation detected along the excitation axis. A Helmholtz coil was used to cancel the earth's magnetic field in (A) and (B) but not in (C), resulting in a small 'antiphase' peak in the upper panel of (C). The asymmetric lineshape of some of the multi-line spectra is due to small imperfections in the crystal.

tion, as depicted in Fig. 6A, the single peak splits into four lines in the presence of an external magnetic field. As expected, for two-photon excitation with crossed-coil detection, no signal is observed in the absence of an external field whereas a symmetric set of lines appears when a field is applied obliquely to the quadrupolar symmetry axis (Fig. 6B). When repeated with excitation and detection in a single doubly tuned RF coil (Fig. 6C), a set of lines appears when an external field is applied but this time is antisymmetric with respect to zero frequency. The symmetries of the spectra confirm that the signal does indeed appear along an axis perpendicular to the excitation axis. The fact that in Fig. 6B the two doublets have opposite sign is a reflection of the excitation geometry which should result in no observable signal as the magnetic field is turned off and the lines collapse together.

Alternatively, it would be possible to observe the double-quantum coherences in the absence of an external magnetic field with a two-pulse experiment in which two-photon excitation was followed by an on-resonance pulse with phase cycling or field gradients applied to select out double-quantum contributions to the signal. In fact this has been done previously by Gold and Hahn [7] for the case of a spin-3/2 nucleus in a strong magnetic field where double-quantum coherence between the $|3/2\rangle$ and $|-1/2\rangle$ states was excited by irradiation at half the transition frequency, which did not correspond to on-resonance excitation involving the intermediate $|1/2\rangle$ state because of the quadrupole interaction. Zur and Vega [16] similarly demonstrated double-quantum coherence in a spin-1 nucleus. In both instances, RF was applied along an axis perpendicular to the external magnetic field so that only $\Delta m = \pm 2$ transitions were allowed by absorption of two transverse photons.

Excitation of $|\Delta m| > 1$ coherences by absorption of multiple transverse photons is interesting from the point of view of exciting higher order multiple-quantum coherences. Such excitation is not limited to single spins or to quadrupolar systems and has previously been achieved in dipolar coupled spin systems [32]. However, since the multi-photon excitation efficiency decreases exponentially with the number of photons involved, other techniques such as multiple pulse sequences [33] have proven more efficient and are used widely today. Furthermore, because multiple-quantum coherences are not directly observable in a standard NMR experiment, the advantages of off-resonance excitation, namely detection during excitation, do not extend to any such coherences that may be excited. It is the practical advantages of detection outside the excitation bandwidth that have fueled our recent interest in multi-photon excitation in NMR [10,18] and NQR [11], and it is in this respect that we expect two-photon excitation to find practical application.

The generality of the technique in NQR will be limited by the fact that, in the experiment which we present here, the two-photon excited NQR signal arising from a powder sample averages to zero as a consequence of the angular dependence of Eq. (13). Furthermore, the weak nutation rates achieved in our experiments result in a very limited excitation bandwidth if 90° pulses are required. This latter difficulty can be overcome by combining two-photon NQR with noise spectroscopy [34,35], where small tip angle pulses provide a broad excitation bandwidth even with low nutation frequencies. In addition, application of two-photon NQR to samples with smaller quadrupole couplings (or larger γ) will improve the nutation rate, as will improvements in RF field

strengths made possible by developments with microcoils, being developed in our lab and elsewhere [36]. Further improvements may also be achieved with two-color excitation using two independent RF fields whose frequencies sum to or differ by the resonance frequency [18].

5. Conclusions

We have applied an average Hamiltonian treatment to two-photon excitation of NQR in a spin-3/2 system, predicting that excitation at half the normal resonance frequency produces single-quantum coherences (via absorption of one longitudinal and one transverse photon), double-quantum coherences (via absorption of two transverse photons), and a resonance offset analogous to the Bloch–Siegert shift in NMR. We have demonstrated two-photon excitation in a single crystal of potassium chlorate, and have observed the single- and double-quantum coherences directly. We verified the angular dependence of the nutation rate on RF coil orientation and demonstrated that signal appears along an axis perpendicular to the RF field.

Acknowledgments

This work was supported by a grant from the Natural Sciences and Engineering Research Council (NSERC) of Canada. P.E. thanks NSERC and the Paetzold Trust for post-graduate scholarships. We thank Dr. Kim Wong (UBC Liposomes Research Unit) for for his assistance with the MSL200.

Appendix A. Spin-3/2 with non-zero asymmetry parameter

For the case of a non-zero asymmetry parameter ($\eta \neq 0$), the quadrupolar Hamiltonian of a single spin-3/2 nucleus in an electric field gradient, written in the Zeeman basis is

$$\mathcal{H}_Q = \frac{\omega_Q}{2}\begin{pmatrix} 1 & 0 & \kappa & 0 \\ 0 & -1 & 0 & \kappa \\ \kappa & 0 & -1 & 0 \\ 0 & \kappa & 0 & 1 \end{pmatrix}. \tag{A.1}$$

The quadrupolar Hamiltonian can be diagonalized using the matrix

$$A = \frac{1}{2\xi(\xi-1)}\begin{pmatrix} \kappa & 0 & \xi-1 & 0 \\ 0 & \kappa & 0 & 1-\xi \\ 1-\xi & 0 & \kappa & 0 \\ 0 & \xi-1 & 0 & \kappa \end{pmatrix} \tag{A.2}$$

becoming

$$\mathcal{H}'_Q = A^{-1}\mathcal{H}_Q A = \frac{\omega'_Q}{2}\begin{pmatrix} 1 & & & \\ & -1 & & \\ & & -1 & \\ & & & 1 \end{pmatrix}. \tag{A.3}$$

Thus, for $\eta \neq 0$, the asymmetry parameter increases the level splitting by a factor ξ. The spin operators in this new basis are

$$I'_x = c_{0x}I_x^{1-2} + c_{1x}I_x^{3-4} + c_{2x}I_x^{1-4} + c_{3x}I_x^{2-3}, \tag{A.4}$$

$$I'_y = c_{0y}I_y^{1-2} + c_{1y}I_y^{3-4} + c_{2y}I_y^{1-4} + c_{3y}I_y^{2-3}, \tag{A.5}$$

$$I'_z = c_{0z}I_x^{2-4} + c_{1z}I_x^{1-3} + c_{2z}I_z^{1-4} + c_{3z}I_z^{2-3}, \tag{A.6}$$

where Table A.1 in this Appendix summarizes the coefficients used above. The expansion is unique except for terms in I_z^{r-s} which can be expanded in terms of linear combinations of $I_0^{r'-s'}$ and $I_z^{r''-s''}$.

From here, we proceed as in the case of $\eta = 0$ by choosing an interaction representation, $U = e^{i\mathcal{H}'_Q t}$, that removes the diagonal quadrupolar Hamiltonian. By taking advantage of the commutation relations of fictitious spin-1/2 operators, we write the effective Hamiltonian in this interaction representation as

$$\mathcal{H}'_{\text{eff}}(t) = \begin{pmatrix} \omega_z \begin{pmatrix} c_{0z}\left\{I_x^{2-4}\cos\omega'_Q t - I_y^{2-4}\sin\omega'_Q t\right\} \\ +c_{1z}\left\{I_x^{1-3}\cos\omega'_Q t + I_y^{1-3}\sin\omega'_Q t\right\} \\ +c_{2z}I_z^{1-4} + c_{3z}I_z^{2-3} \end{pmatrix} \\ +\omega_y \begin{pmatrix} c_{0y}\left\{I_y^{1-2}\cos\omega'_Q t - I_x^{1-2}\sin\omega'_Q t\right\} \\ +c_{1y}\left\{I_y^{3-4}\cos\omega'_Q t + I_x^{3-4}\sin\omega'_Q t\right\} \\ +c_{2y}I_y^{1-4} + c_{3y}I_y^{2-3} \end{pmatrix} \\ +\omega_x \begin{pmatrix} c_{0x}\left\{I_x^{1-2}\cos\omega'_Q t + I_y^{1-2}\sin\omega'_Q t\right\} \\ +c_{1x}\left\{I_x^{3-4}\cos\omega'_Q t - I_y^{3-4}\sin\omega'_Q t\right\} \\ +c_{2x}I_x^{1-4} + c_{3x}I_x^{2-3} \end{pmatrix} \end{pmatrix} \cos\omega_{\text{RF}} t. \tag{A.7}$$

Calculation of first order terms in the Magnus expansion requires keeping track of $18^2 = 324$ terms, each of which contains a commutation and a temporal integral over trigonometric functions. Fortunately, the latter factor comes in nine varieties, five of which vanish as summarized in Table II in [18]. The non-vanishing first order terms in the Magnus expansion for $\omega_{\text{RF}} = \omega'_Q/2$

Table A.1
Coefficients used in expansion of spin operators to fictitious spin-1/2 basis

i	c_{0i}	c_{1i}	c_{2i}	c_{3i}
x	$\frac{\sqrt{3}+\kappa}{\xi}$	$\frac{\sqrt{3}+\kappa}{\xi}$	$\frac{\sqrt{3}\kappa-1+\xi}{\xi}$	$\frac{-\sqrt{3}\kappa+1+\xi}{\xi}$
y	$\frac{\sqrt{3}-\kappa}{\xi}$	$\frac{\sqrt{3}-\kappa}{\xi}$	$\frac{\sqrt{3}\kappa+1-\xi}{\xi}$	$\frac{\sqrt{3}\kappa+1+\xi}{\xi}$
z	$\frac{2\kappa}{\xi}$	$-\frac{2\kappa}{\xi}$	$\frac{1}{\xi}(\xi+2)$	$-\frac{1}{\xi}(\xi-2)$

(expressed in the original Zeeman basis) are given by Eq. (14).

Although evolution under the full two-photon excitation Hamiltonian is non-trivial, some insight can be gained by considering only short pulses ($\mathcal{H}^{(1)}\tau \ll 1$) so that each term in Eq. (14) contributes independently to the signal. According to Eq. (11), using the Hamiltonian of Eq. (14), the free induction signal in the quadrupolar PAS is

$$\langle \vec{I} \rangle \propto \begin{pmatrix} -\omega_y\omega_z(\eta^2+2\eta-3) \\ \omega_x\omega_z(\eta^2-2\eta-3) \\ \omega_x\omega_y 4\eta \end{pmatrix} \frac{\tau\cos\omega'_Q t}{2(1+\frac{\eta^2}{3})\omega'_Q}. \qquad \text{(A.8)}$$

The x-, y-, and z-components are due to the third, second, and fourth terms in Eq. (14) respectively, whereas the first and fifth terms produce no observable signal. As in the $\eta = 0$ case, this signal appears perpendicular to the excitation coil axis, shown by the vanishing of the dot product of Eq. (A.8) with the unit vector defining the excitation coil axis ($(\omega_x, \omega_y, \omega_z)/(\gamma B_1)$).

References

[1] F.H.M. Faisal, Theory of Multiphoton Processes, Plenum Press, New York, 1987.

[2] J. Winter, Etude de transitions faisant intervenir plusieurs quanta entre deux niveaux atomiques, C. R. Acad. Sci. (Paris) 241 (1955) 375–377.

[3] R. Boscaino, I. Ciccarello, C. Cusumano, M.W.P. Strandberg, Second-harmonic generation and spin decoupling in resonance two-level spin systems, Phys. Rev. B 3 (8) (1971) 2675–2682.

[4] W.A. Anderson, Nuclear resonance saturation effects and multiple-quantum transitions, Phys. Rev. 104 (1956) 850–851.

[5] J.I. Kaplan, S. Meiboom, Double-quantum transitions in nuclear magnetic resonance spectra of liquid, Phys. Rev. 106 (1957) 499–501.

[6] B.W. Shore, The Theory of Coherent Atomic Excitation, Wiley, New York, 1990.

[7] D.G. Gold, E.L. Hahn, Two-photon transient phenomena, Phys. Rev. A 16 (1) (1977) 324–326.

[8] R. Boscaino, G. Messina, Double quantum coherent transients in a two-level spin system: a vectorial model, Physica C 138 (1986) 179–187.

[9] M. Kalin, I. Gromov, A. Schweiger, Transparency in two-level spin systems induced by a longitudinal field, Phys. Rev. A 69 (2004) 033809.

[10] C.A. Michal, Nuclear magnetic resonance noise spectroscopy using two-photon excitation, J. Chem. Phys. 118 (8) (2003) 3451–3454.

[11] P.T. Eles, C.A. Michal, Two-photon excitation in nuclear quadrupole resonance, Chem. Phys. Lett. 376 (2003) 268–273.

[12] P. Bucci, M. Martinelli, S. Santucci, Response to double irradiation of a nuclear spin system: general treatment and new multiple quantum transitions, J. Chem. Phys. 53 (12) (1970) 4524–4531.

[13] F. Chiarini, M. Martinelli, L. Pardi, S. Santucci, Electron-spin double resonance by longitudinal detection: lineshape and many-quantum transitions, Phys. Rev. B 12 (3) (1975) 847–852.

[14] J.H. Shirley, Solution of the Schrödinger equation with a Hamiltonian periodic in time, Phys. Rev. 138 (1965) B979–B987.

[15] Y. Zur, M.H. Levitt, S. Vega, Multiphoton NMR spectroscopy on a spin system with $I = 1/2$, J. Chem. Phys. 78 (9) (1983) 5293–5310.

[16] Y. Zur, S. Vega, Two-photon NMR on spins with $I = 1$ in solids, J. Chem. Phys. 79 (2) (1983) 548–558.

[17] I. Gromov, A. Schweiger, Multiphoton resonances in pulse EPR, J. Magn. Reson. 146 (2000) 110–121.

[18] P.T. Eles, C.A. Michal, Two-photon two-color nuclear magnetic resonance, J. Chem. Phys. 121 (2004) 10167–10173.

[19] U. Haeberlen, J.S. Waugh, Coherent averaging effects in magnetic resonance, Phys. Rev. 175 (1968) 453–467.

[20] M. Ito, N. Mikami, Multi-photon spectroscopy, Appl. Spectrosc. Rev. 16 (1980) 299–352.

[21] G. Goelman, D.B. Zax, S. Vega, Observation of three-photon resonance in NMR under four-field irradiation, J. Chem. Phys. 87 (1) (1987) 31–44.

[22] K.L. Sauer, B.H. Suits, A.N. Garroway, J.B. Miller, Three-frequency nuclear quadrupole resonance of spin-1 nuclei, Chem. Phys. Lett. 342 (2001) 362–368.

[23] K.L. Sauer, B.H. Suits, A.N. Garroway, J.B. Miller, Secondary echoes in three-frequency nuclear quadrupole resonance of spin-1 nuclei, J. Chem. Phys. 118 (2003) 5071–5081.

[24] S. Vega, Fictitious spin-1/2 operator formalism for multiple quantum NMR, J. Chem. Phys. 68 (12) (1978) 5518–5757.

[25] W. Magnus, On the exponential solution of differential equations for a linear operator, Commun. Pure Appl. Math. 7 (1954) 649–673.

[26] F. Bloch, A. Siegert, Magnetic resonance for nonrotating fields, Phys. Rev. 57 (1940) 522–527.

[27] J. Danielsen, A. Hazell, F.K. Larsen, The structure of potassium chlorate at 77 and 298 K, Acta Cryst. B 37 (1981) 913–915.

[28] H. Zeldes, R. Livingston, Zeeman effect on the quadrupole spectra of sodium, potassium and barium chlorates, J. Chem. Phys. 26 (1957) 1102–1106.

[29] C. Michal, K. Broughton, E. Hansen, A high performance digital receiver for home-built nuclear magnetic resonance spectrometers, Rev. Sci. Instrum. 73 (2002) 453–458.

[30] T. Kushida, G.B. Bendek, N. Bloembergen, Dependence of the pure quadrupole resonance frequency on pressure and temperature, Phys. Rev. 104 (1956) 1364–1377.

[31] A. Abragam, Principles of Nuclear Magnetism, Oxford University Press, Oxford, 1961.

[32] G. Drobny, A. Pines, S. Sinton, D. Weitekamp, D. Wemer, Fourier transform multiple quantum nuclear magnetic resonance, Faraday Div. Chem. Soc. 13 (1979) 49–174.

[33] G. Bodenhausen, Multiple-quantum NMR, Prog. Nucl. Magn. Reson. Spectrosc. 14 (1981) 137–173.

[34] R.R. Ernst, Magnetic resonance with stochastic excitation, J. Magn. Reson. 3 (1970) 10–27.

[35] R. Kaiser, Coherent spectrometry with noise signals, J. Magn. Reson. 3 (1970) 28–43.

[36] K. Yamauchi, J.W.G. Janssen, A.P.M. Kentgens, Implementing solenoid microcoils for wide-line solid-state NMR, J. Magn. Reson. 167 (2003) 87–96.